[17] B. Moghaddam, T. Jebara, and A. Pentland, "Bayesian face recognition," *Pattern Recognit.*, vol. 33, no. 11, pp. 1771–1782, Nov. 2000.
[18] A. Nefian, "A hidden Markov model-based approach for face detection and recognition," Ph.D. dissertation, Dept. Elect. Comput. Eng. Elect. Eng., Georgia Inst. Technol., Atlanta, 1999.
[19] P. J. Phillips *et al.*, "Overview of the face recognition grand challenge," presented at the IEEE CVPR, San Diego, CA, Jun. 2005.
[20] H. T. Tanaka, M. Ikeda, and H. Chiaki, "Curvature-based face surface recognition using spherical correlation-principal direction for curved object recognition," in *Proc. Int. Conf. Automatic Face and Gesture Recognition*, 1998, pp. 372–377.
[21] M. Turk and A. Pentland, "Eigenfaces for recognition," *J. Cognit. Sci.*, pp. 71–86, 1991.
[22] V. N. Vapnik, *Statistical Learning Theory*. New York: Wiley, 1998.
[23] W. Zhao, R. Chellappa, A. Rosenfeld, and P. Phillips, "Face recognition: A literature survey," *ACM Comput. Surveys*, vol. 35, no. 44, pp. 399–458, 2003.
[24] W. Zhao, R. Chellappa, and P. J. Phillips, "Subspace linear discriminant analysis for face recognition," UMD TR4009, 1999.

Face Verification Using Template Matching

Anil Kumar Sao and B. Yegnanarayana

***Abstract*—Human faces are similar in structure with minor differences from person to person. These minor differences may average out while trying to synthesize the face image of a given person, or while building a model of face image in automatic face recognition. In this paper, we propose a template-matching approach for face verification, which neither synthesizes the face image nor builds a model of the face image. Template matching is performed using an edginess-based representation of the face image. The edginess-based representation of face images is computed using 1-D processing of images. An approach is proposed based on autoassociative neural network models to verify the identity of a person. The issues of pose and illumination in face verification are addressed.**

***Index Terms*—Autoassociative neural network (AANN), face verification, 1-D image processing.**

I. Introduction

The objective of the face verification task is to accept or reject the identity claim of the person using his or her face image [1]. The issues involved in this task can be categorized into two classes, namely, 1) interclass variation and 2) intraclass variation. The interclass variation refers to the differences in the face images of two people, which are due to uniqueness of the features present in the face image of each person. The intraclass variation refers to the differences in the face images of a given person under varying conditions of pose, illumination, and expressions [1].

Template matching is one of the approaches proposed in the literature to address the issue of interclass variation [2], because it takes the unique information of a person's face image into account. But this approach has the drawback that it gives poor performance under intraclass variation [3]. The problem of intraclass variation can be overcome using an approach which synthesizes a 3-D model of the face image from a given sample [4]–[8]. But the synthesis of face image may result in some artifacts and some loss of the unique information. Thus, the synthesis-based approach may degrade the performance of the face verification system. Another way to address the issue of intraclass variation is to consider several reference face images which capture variations in the face images, such as different poses or due to different lighting conditions. These reference face images can be used to build a model for that person's face image. The model is used to verify the identity of a test face image. Such methods are discussed in [9]–[14]. In these cases, the model may average out some of the information that is unique for that person.

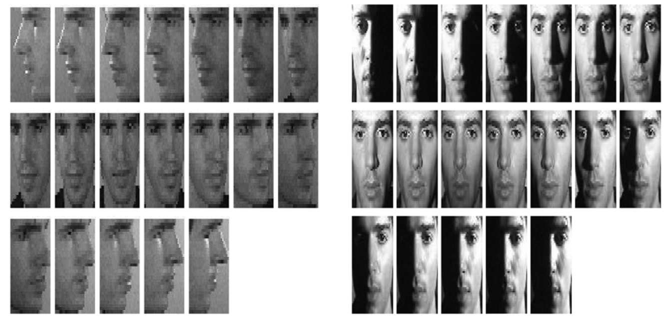

(a) (b)

Fig. 1. Face images of a person with (a) pose variation and (b) illumination variation.

In this paper, we propose a template-matching-based approach, which neither synthesizes the face image nor derives a model for the person's face. We use reference face images (at different poses or at different lighting conditions) separately for template matching. The template matching is performed using an edginess-based representation of a face image [15]. The scores obtained by template matching with different reference images are combined in a selective way. The combined scores are used for verification by using the autoassociative-neural-network (AANN) model-based classifier.

The performance of the proposed approach is evaluated on the FacePix database collected at Arizona State University [16], [17]. The FacePix database consists of 30 people, each having two sets of face images: A set with pose-angle variation, and a set with illumination angle variation. The set with pose-angle variations has 181 images (representing angles from -90° to 90° at 1° interval). In this paper, we denote these images by $I^1, \ldots, I^{181}$. The illumination set is captured with the subject looking directly into the camera while the light source is moved around the subject. The light source moves at a 1° interval from -90° to 90°. These images are denoted by $L^1, \ldots, L^{181}$. Some of the face images of a person are shown in Fig. 1. In our experiments, the size of the face images is rescaled to 30×30 pixels.

The organization of this paper is as follows. Section II explains the template matching using the edginess-based representation of a face image. The scores obtained by matching several templates are combined in a selective way as explained in Section III. An approach is proposed in Section IV to classify the combined scores using AANN models. Experimental results are discussed in Section V, and a summary of the work is given in Section VI.

Manuscript received November 1, 2006; revised May 10, 2007. The associate editor coordinating the review of this manuscipt and approving it for publication was Prof. Rama Chellappa.

A. K. Sao is with the Department of Computer Science and Engineering, Indian Institute of Technology-Madras, Chennai 600 036, India (e-mail: anil@cs.iitm.ernet.in).

B. Yegnanarayana is with the International Institute of Information Technology, Hyderabad 500 032, India (e-mail: yegna@iiit.ac.in).

Color versions of one or more of the figures in this paper are available online at http://ieeexplore.ieee.org.

Digital Object Identifier 10.1109/TIFS.2007.902920

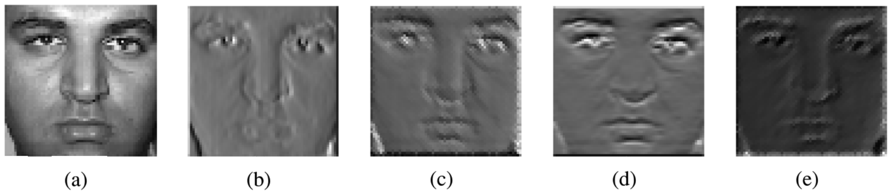

Fig. 2. (a) Gray-level image. Edge gradient (i_θ^g) of the face image obtained for (b) $\theta = 0°$, (c) $\theta = 45°$, (d) $\theta = 90°$, and (e) $\theta = 135°$.

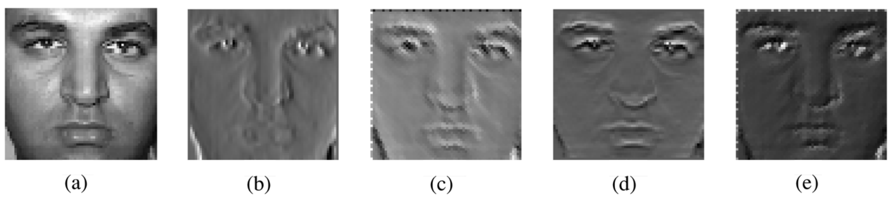

Fig. 3. (a) Gray-level image. Potential field (u_θ) developed from the edge gradient of the face image (a), for (b) $\theta = 0°$, (c) $\theta = 45°$, (d) $\theta = 90°$, and (e)$\theta = 135°$.

II. Template Matching

Template matching is performed using a correlation-based technique. The correlation between the reference face image $r(x, y)$ and test face image $i(x, y)$ is computed as follows:

$$\begin{aligned} c(\tau_x, \tau_y) &= i(x, y) \odot r(x, y) \\ &= \int\int i(x, y) r(x + \tau_x, y + \tau_y) dx dy \\ &= \int\int I^*(u, v) R(u, v) \exp(j2\pi(u\tau_x + v\tau_y)) du dv \end{aligned} \quad (1)$$

where $I(u, v)$ and $R(u, v)$ are the Fourier transforms of $i(x, y)$ and $r(x, y)$, respectively, and $\odot$ denotes the correlation operator. The correlation output $c(\tau_x, \tau_y)$ should have a high value at the origin, when the test and reference face images are similar. On the other hand, if the test and reference face images are not similar, then the correlation output should have a relatively low value even at the origin. Here, the origin refers to the center of the correlation output. The relative heights of the values at the origin determine whether the test and reference face images are similar. The correlation output can be quantified using the peak-to-sidelobe ratio (PSR) measure, discussed in [18]. The PSR measures the sharpness of the highest peak in the correlation output. For similar face images, the peak will be sharp and high relative to the values in the neighborhood. Otherwise, the peak will be low and blunt.

A. Template Matching Using Edginess-Based Representation

Cognitive psychological studies [19], [20] indicate that human beings recognize the line sketches as quickly, and almost as accurately, as the gray-level images. This might imply that edge images of faces could be used for face recognition to achieve similar accuracy as the gray-level images. An advantage of the edge map is that it is less sensitive to illumination [21], [22]. Computation of the edge map requires thresholding of the edge gradient values. Since the selection of a threshold value is crucial in deriving the edge map, spurious edges may show up in the edge map for low threshold values. On the other hand, a high threshold value may remove significant edges. Therefore, a continuous edge gradient representation [23] is used in this paper and the edge gradient is computed using 1-D processing of images [24].

In the 1-D processing of a given image, the smoothing operator is applied along one direction, and the derivative operator is applied along the orthogonal direction. By repeating this procedure of smoothing followed by differential operation along two orthogonal directions, two edge gradients are obtained, which together can be used to represent the intensity gradient of the image. Let i_θ^g be the edge gradient obtained by applying the derivative operator along the θ direction with respect to the horizontal scan line. Fig. 2 shows the gradient maps obtained along different directions. It shows that the edge gradients for different values of θ give different information about the same face image. However, the edge gradient representation cannot be used directly for correlation matching because of sparsity [23]. The sparsity issue can be overcome to some extent using the potential field representation discussed in [23]. Let u_θ be the potential field derived from the edge gradient i_θ^g. The potential fields obtained for different directions are shown in Fig. 3. Although the edges appear smeared in the potential field representation, it may still improve the correlation between the face images of the same person, even if there is some deviation in the edge contours of the two images. The edge gradients (i_θ^g) for different directions (θ) give different information about the face image. Hence, we have performed template matching between partial evidence (u_θ) of the given test and reference face images. Let c_θ be the correlation output for the partial evidence along the θ direction. The correlation output is used to compute the PSR (P_θ). Ideally, the P_θ should be high if the given test face image is similar to the reference image.

In our experiment, we have computed the partial evidence (u_θ) along four directions $\theta = 0°, 45°, 90°$, and $180°$. Hence, for a given test face image, a four-dimensional feature vector (four PSR values) is obtained. Fig. 4(a) shows the scatter plot obtained from the PSR vectors of the true class and false class face image for a person using pose variation set. For visualization, we show the plot using three ($\theta = 0°, 45°$, and $90°$) of the four dimensions. In this example, we have used I^1 as a reference face image of a person. The remaining 180 face images of the given person form examples of the true class image, and the corresponding PSR values are denoted by diamond $(\diamond)$ symbol in the plot. For the false class, $29 \times 181 = 5249$ face images are available, and the corresponding PSR values are shown by point $(\cdot)$ symbol in the scatter plot. Although the separation between the true and false class face images is not decisive, one can observe from the plot that high scores are given by the face images I^2, I^3, I^4, I^5, and I^6 of the true class. These face images have pose that is close to the pose of the reference face image. One can also see that none of the face images of the false class gives high scores. It means that the chances of matching face images of two different people even with the same pose are less. Similar observations can be made from the scatter plot shown in Fig. 4(b), which is obtained using I^{46} as the reference face image. The behavior of the scatter plots is utilized to develop a method for face verification.

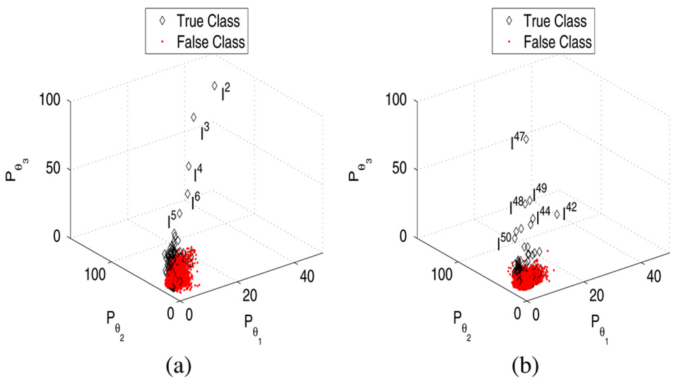

Fig. 4. Scatter plot of a person using potential field representation, obtained from $\theta_1 = 0°, \theta_2 = 45°, \theta_3 = 90°$, and using reference face image as I^1 in (a) and I^{46} in (b).

III. Combining Scores From Different Templates

One can conclude from the previous section that if a test face image of the true class has a pose that lies in the neighborhood poses of the two reference face images, then the test image will give high scores with respect to both reference face images. It is better to combine these scores rather than use them separately for making a decision. One way to combine the scores is as follows. Let $P_\theta^{t,l}$ be the similarity score (PSR) obtained when the potential field representation along the θ direction of the test face image I^t is correlated with the corresponding representation of the reference image I^l. The combined similarity score for two reference images I^l and I^m is given by

$$P_\theta^{t,l,m} = \left[\frac{1}{2}\left[\left(P_\theta^{t,l}\right)^n + \left(P_\theta^{t,m}\right)^n\right]\right]^{\frac{1}{n}} \tag{2}$$

where the parameter n decides the weights associated with the scores. For $n \leq 1, \min[P_\theta^{t,l}, P_\theta^{t,m}] \leq P_\theta^{t,l,m} \leq (P_\theta^{t,l} + P_\theta^{t,m})/2$, and for $n \geq 1, (P_\theta^{t,l} + P_\theta^{t,m})/2 \leq P_\theta^{t,l,m} \leq \max[P_\theta^{t,l}, P_\theta^{t,m}]$. A low value of n is suitable for false class, and a high value of n is for true class. One has to choose a value of n to enhance the separation between the true and false classes. We have found empirically that $n = 3$ is a good choice. Fig. 5 illustrates the effect of n on the PSR vectors in the scatter plots. The scatter plots in the Fig. 5(a) and (b) are the same as shown in Fig. 4(a) and (b), but with a different view angle. In this example, we have shown the scores from the true-class face images I^t for $2 \leq t \leq 45$. Fig. 5(c)–(f) are the scatter plots obtained after combining the PSR scores in Fig. 5(a) and (b) using (2), for $n = 0.4, 1, 3$, and 5, respectively. One can see that as n increases, the points due to true and false classes move away from the origin. Similarly, we can also combine the scores obtained from other reference face images of adjacent poses.

IV. Classification Using AANN Models

The next task is to classify a given test face image using the feature vectors consisting of the combined score $P_\theta^{t,l,m}$ for the four different values of θ. One can employ a classifier based on a multilayer-perceptron (MLP) [25] neural network model or a support vector machine (SVM) [26]. But these models require samples from both the true and false classes. Though we can have a large number of false class images for a given person, we may not have that many face images of the true class. This problem can be overcome by using an approach for classification based on the AANN model. There are two reasons for adopting this approach. First, one can generate many face images of the false class for a given person. Second, the feature points due to the false class are more clustered compared to the feature points due to the true class in the scatter plots. The distribution of these clustered points of the false class can be modeled using the distribution capturing ability of an AANN [27] model. The distribution of points due to the false class could be different for different reference face images. Hence, separate AANN models are used for each reference face image. The AANN model is used for accepting or rejecting a claim. When a test face image belonging to the true class is given to the AANN model, the resulting score vector does not fall into the cluster of points belonging to the false class. Thus, using a suitable threshold for the output of the AANN model, a decision can be made to accept or reject the claim of the test input.

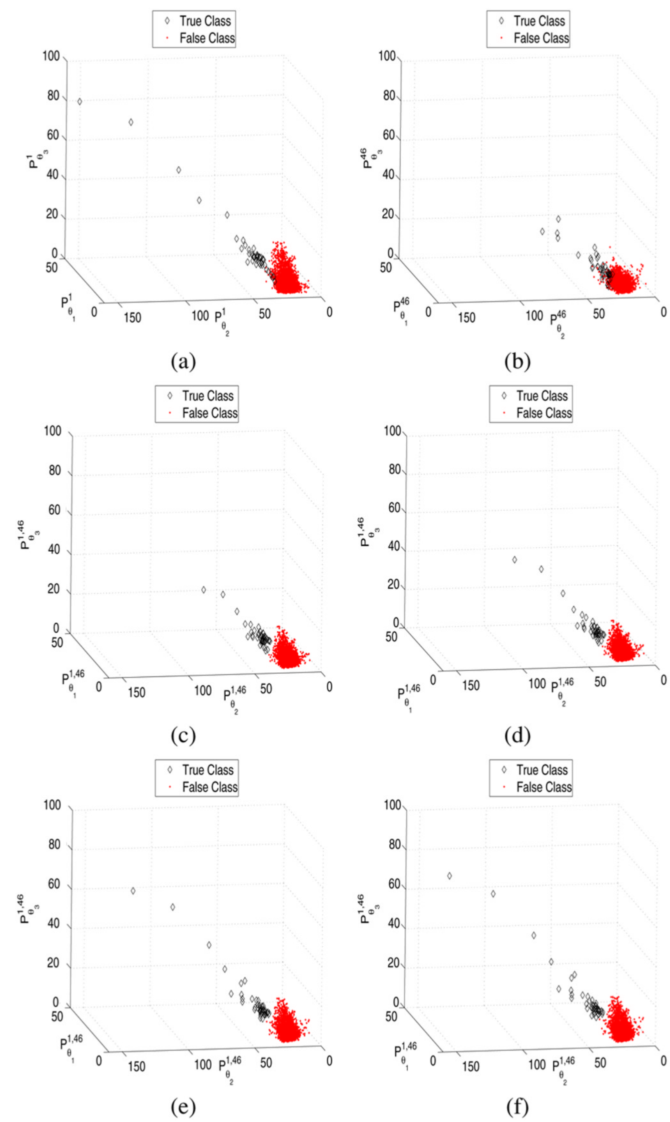

Fig. 5. Scatter plot of a person using potential field representation for (a) reference image as I^1 and for (b) reference image I^{46}, using $\theta_1 = 0°, \theta_2 = 45°, \theta_3 = 90°$. Combining (a) and (b) using (2) for (c) $n = 0.4$, (d) $n = 1$, (e) $n = 3$, and (f) $n = 5$.

V. Experimental Results

Face verification experiments were performed using a set of face images with pose variation and a set of face images with illumination variation separately. The results on the pose variation set are explained first. The block diagram of the training phase is shown in Fig. 6. In

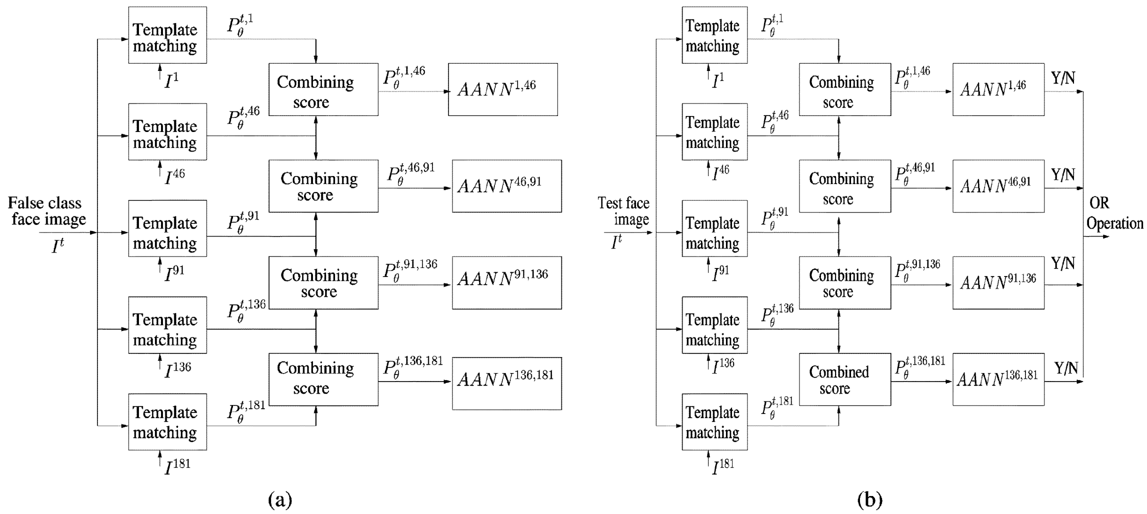

Fig. 6. Block diagram of face verification system for (a) training phase and (b) testing phase.

this diagram, we have shown training with five reference face images $I^1, I^{46}, I^{91}, I^{136}$ and I^{181}. The process can be generalized for any number of reference face images. The reference face images are chosen in such a way that their poses are uniformly spaced over the span of $1^\circ - 181^\circ$. Several false class images are considered, and their potential field representations (u_θ) are computed along four directions ($\theta = 0^\circ, 45^\circ, 90^\circ$, and 135°). The correlation output of each representation with the corresponding representation of each reference face image is used to compute the similarity score (PSR). Five sets of four-dimensional feature vectors (four PSR values) are obtained for each image from the false class. The scores obtained from two reference face images with adjacent poses are combined using (2), as shown in Fig. 6(a). The combined scores are presented to an AANN model for training. Let $\mathrm{AANN}^{1,46}$ denote the AANN model trained with the combined similarity scores $(P_\theta^{t,1,46})$ obtained using the reference face images I^1 and I^{46}. The structure of the AANN model is $4L8N2N8N4L$, where L refers to a linear unit, and N refers to a nonlinear unit. The AANN model is trained using the backpropagation algorithm for about 3000 epochs. Similarly, the models $\mathrm{AANN}^{46,91}, \mathrm{AANN}^{91,136}$ and $\mathrm{AANN}^{136,181}$ are obtained for the same false-class face images. The block diagram for the testing phase of the face verification system is shown in Fig. 6(b). For a given test face image, the potential field representation u_θ is computed along the four directions ($\theta = 0^\circ, 45^\circ, 90^\circ$, and 135°). The correlation output of each representation with the corresponding representation of each reference face image of the claimed identity is computed. The scores are combined as in the training phase, and are presented to the AANN models as shown in Fig. 6(b). The combined similarity score (4-D feature vector) is used to compute the error in associating the vector with each AANN model corresponding to the reference face images. If the error is above a threshold in any one of the AANN models, the claim is accepted. Note that the threshold value for each AANN model is different. The false acceptance ratio (FAR) and false rejection ratio (FRR) are two error metrics that are used to evaluate the face verification system. The tradeoff between FAR and FRR is a function of the decision threshold. The equal error rate (EER) is the value for which the error rates FAR and FRR are equal. The computation of EER for a single person is as follows: Note that $I^1, I^{46}, I^{91}, I^{136}$, and I^{181} are used as reference face images. The remaining $176 = (181 - 5)$ face images form the examples of the true class. For false class, $5249 = (29 \times 181)$ face images are available. Out of these, 2900 face images are used to train the models $\mathrm{AANN}^{1,46}, \mathrm{AANN}^{46,91}, \mathrm{AANN}^{91,136}$, and $\mathrm{AANN}^{136,181}$. The remaining $2349 = (5249 - 2900)$ false class face images are used for testing. The true class samples for each AANN model consist of the true class face images with poses in a specific range. For example, for the model $\mathrm{AANN}^{1,46}$, the true class samples are the images in the range I^1 to I^{46}. By varying the threshold value of the $\mathrm{AANN}^{1,46}$, the receiver operating characteristics (ROC) curve is obtained as shown in Fig. 7. The ROC characteristics show that the FAR curve is steep, indicating that the corresponding combined PSR values are clustered around low values. On the other hand, the FRR curve is slowly varying, indicating that the corresponding PSR values are scattered more. The intersecting point of the FAR and FRR curve gives the EER for this model. Likewise, the EERs for the other AANN models are computed, and the average of EER is obtained for that person. The experiment is repeated by building the verification model for each person, and the corresponding value of EER is used as a measure of performance. The average EERs obtained for the pose variation set of the FacePix database [16], [17] for one, three, and five reference templates cases are 51%, 34.55%, and 14.17%, respectively. Likewise, the average EERs obtained for the illumination variation set of the FacePix database [16], [17] for one, three, and five reference templates are 33%, 16.24%, and 3.5%, respectively. For the pose subset of the CMU, pose, illumination, and expression (PIE) database [28], an average EER of 43.40% was obtained using single reference templates.

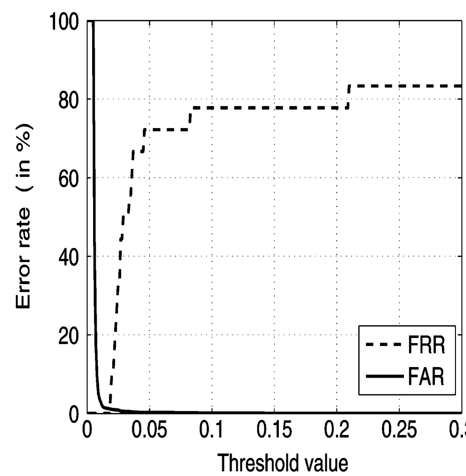

Fig. 7. ROC curves for a person using $\mathrm{AANN}^{1,46}$.

For a comparison of results with other studies on these databases, an identification system was developed using the verification models.

TABLE I
AVERAGE RECOGNITION RATE (IN %) FOR DIFERENT SETS OF REFERENCE FACE IMAGES UNDER POSE VARIATIONS

Set of reference face images	I^{91}	I^1, I^{91}, and I^{181}	I^1, I^{46}, I^{91}, I^{136}, and I^{181}
PCA	20.74	50.53	71.66
LDA	20.70	56.92	78.67
HMM	31.68	41.27	63.50
BIC	18.42	45.19	69.47
Proposed approach	**46.19**	**74.39**	**92.23**

TABLE II
AVERAGE RECOGNITION RATE (IN %) FOR DIFERENT SETS OF REFERENCE FACE IMAGES UNDER ILLUMINATION VARIATIONS

Set of reference face images	L^{91}	L^1, L^{91}, and L^{181}	L^1, L^{46}, L^{91}, L^{136}, and L^{181}
PCA	48.84	71.71	90.33
LDA	53.04	79.52	94.92
HMM	19.26	37.38	59.37
BIC	49.80	79.10	93.54
Proposed approach	**81.43**	**94.32**	**99.72**

TABLE III
AVERAGE RECOGNITION RATE (IN %) ON PIE DATABASE USING A SINGLE FACE IMAGE FOR TRAINING

	Eigenfaces	FaceIt	Eigen Light-Fields	Proposed approach
Average recognition	16.6	24.3	52.5	**57.3**

The identification is accomplished by verification on a closed set of test samples. We call the set of all test samples accepted by any of the verification models as the closed set data. The percentage identification for this set is compared with the identification results by other methods reported in the literature [16]. Table I shows the performance of the identification system in comparison with other systems for different sets of reference images. The proposed method seems to perform better than the existing methods. The reason could be that the proposed method may be preserving some unique information of a person's face image for a given pose.

The experiments were repeated with the set of images corresponding to the variation of illumination angle in the FacePix database. The performance for these cases is shown in Table II along with the performance figures using some of the existing methods [16]. The proposed system seems to work better even for different lighting conditions. The results in Tables I and II show that it may be better to use reference face images separately, rather than building a single model from them.

The proposed approach is also evaluated for the pose subset of the CMU, PIE database [28]. The average recognition rate using one reference template is shown in Table III along with the performance obtained using some existing methods [29]. The results show that the proposed method performs better than the existing methods. The performance can be improved further by increasing the number of reference templates. But selection of the reference template is crucial. When three reference templates (frontal view, left profile, and right profile) are used, the average recognition rate increases to 74.69%.

VI. SUMMARY

We have proposed a method to address the pose and illumination problem in face verification. The method uses the given reference face images separately for template matching instead of building a single model, or synthesizing a face image. The template matching is performed using a correlation of images represented by the edge gradient. The edge gradient representation was derived using 1-D processing of images, to derive multiple (partial) evidences for a given image. A method was proposed to combine the scores obtained for different face images. The combined scores were used to verify the identity claim of a person using an AANN model. The AANN model is used to capture the distribution of the false class images and, hence, does not require many reference images of the true class. Experimental results show that the proposed method is a promising alternative to other methods for dealing with the problem of pose and illumination for face verification.

REFERENCES

[1] R. Chellappa, C. Wilson, and S. Sirohey, "Human and machine recognition of faces: A survey," *Proc. IEEE*, vol. 83, no. 5, pp. 705–740, May 1995.
[2] R. Brunelli and T. Poggio, "Face recognition: Features versus templates," *IEEE Trans. Pattern Anal. Mach. Intell.*, vol. 15, no. 10, pp. 1042–1052, Oct. 1993.
[3] A. K. Jain, R. P. W. Duin, and J. Mao, "Statistical pattern recognition: A review," *IEEE Trans. Pattern Anal. Mach. Intell.*, vol. 22, no. 1, pp. 4–37, Jan. 2000.

[4] C. Sanderson, S. Bengio, and Y. Gao, "On transforming statistical models for non-frontal face verification," *Pattern Recognit.*, vol. 39, pp. 288–302, Feb. 2006.
[5] A. S. Georghiades, P. N. Belhumeur, and D. J. Kriegman, "From few to many: Illumination cone models for face recognition under variable lighting and pose," *IEEE Trans. Pattern Anal. Mach. Intell.*, vol. 23, no. 6, pp. 643–660, Jun. 2001.
[6] W. Zhao and R. Chellapa, "SFS based view synthesis for robust face recognition," in *Proc. Int. Conf. Automatic Face and Gesture Recogniton*, Mar. 2000, pp. 285–292.
[7] T. Vetter and V. Blanz, "Estimating coloured 3D face models from single images: An example based approach," in *Proc. Conf. Computer Vision ECCV*, Freiburg, Germany, Jun. 1998, pp. 495–513.
[8] T. Vetter and T. Poggio, "Linear object classes and image synthesis from a single example image," *IEEE Trans. Pattern Anal. Mach. Intell.*, vol. 19, no. 7, pp. 733–742, Jul. 1997.
[9] J. Zhang, Y. Yan, and M. Lades, "Face recognition: Eigenface, elastic graph matching and neural network," in *Proc. IEEE*, Sep. 1997, vol. 85, no. 9, pp. 1423–1435.
[10] O. Deniz, M. Castrilon, and H. M., "Face recognition using independent component analysis and support vector machine," *Pattern Recognit. Lett.*, vol. 22, pp. 2153–2157, 2003.
[11] K. I. Kim, K. Jung, and K. Kim, "Face recognition using support vector machine and with local correlation kernels," *Int. J. Pattern Recognit. Artif. Intell.*, vol. 16, no. 1, pp. 97–111, 2002.
[12] N. Vaswani and R. Chellappa, "Principal component null space analysis for image and video classification," in *IEEE Trans. Image Process.*, Jul. 2006, vol. 15, no. 7, pp. 1816–1830.
[13] M. Savvides, B. V. K. V. Kumar, and P. K. Khosla, "Face verification using correlation filters," in *Proc. 3rd IEEE Automatic Identification Advanced Technologies*, Tarrrytown, NY, Mar. 2002, pp. 56–61.
[14] M. Savvides, B. V. K. V. Kumar, and P. K. Khosla, "Robust shift-invariant biometric identification from partial face images," in *Proc. Biometric Technologies for Human Identification OR51, SPIE Defense and Security Symp.*, Aug. 2004, pp. 124–135.
[15] A. K. Sao and B. Yegnanarayana, "Face verification using correlation filter and auto associative neural netwoks," in *Proc. Int. Conf. Intelligent Sensing and Information Processing*, Chennai, India, Jan. 2004, pp. 364–368.
[16] J. Black, M. Gargesha, K. Kahol, P. Kuchi, and S. Panchanathan, "A framework for performance evaluation of face recogniton algorithm," presented at the ITCOM Internet Multimedia, Boston, MA, Jul. 2002.
[17] G. Little, S. Krisgna, J. Black, and S. Panchanathan, "A methodology for evaluating robustness of face recognition algoritms with respect to change in pose and illumination angle," presented at the IEEE Int. Conf. Acoustics, Speech and Signal Processing, Philadelphia, PA, Mar. 2005.
[18] B. V. K. V. Kumar, M. Savvides, K. Venkataramani, and C. Xie, "Spatial frequency domain image processing for biometric recognition," in *Proc. IEEE Int. Conf. Image Processing*, New York, Sep. 2002, pp. 53–56.
[19] A. Bruce, "The importance of mass in line drawings of faces," *Appl. Cognit. Psychol.*, vol. 6, pp. 619–628, 1992.
[20] I. Biederman and J. Gu, "Surface versus edge-based determinants of visual recognition," *Cognit. Psychol.*, vol. 20, pp. 38–64, 1998.
[21] A. Yilmaz and M. Gokmen, "Eigenhill vs. eigenface and eigenedge," *Pattern Recognit.*, vol. 34, pp. 181–184, Jan. 2000.
[22] Y. Gao and M. K. H. Leung, "Face recognition using line edge map," *IEEE Trans. Pattern Anal. Mach. Intell*, vol. 24, pp. 765–779, Jun. 2002.
[23] A. K. Sao, B. Yegnanarayana, and B. V. K. V. Kumar, "Significance of image representation for face recognition," *Signal Image Video Process.*, to be published.
[24] P. K. Kumar, S. Das, and B. Yegnanarayaiui, "One-dimensional processing of images," presented at the Int. Conf. Multimedia Processing and Systems, Chennai, India, Aug. 2000.
[25] B. Yegnanarayana*, Artificial Neural Networks*. Englewood Cliffs, NJ: Prentice-Hall, 1999.
[26] S. Haykin*, Neural Networks A Comprehensive Foundation*. New York: Macmillan, 1994.
[27] B. Yegnanarayana and S. P. Kishore, "AANN An alternative to GMM for pattern recognition," *Neural Netw.*, vol. 15, pp. 459–469, Apr. 2002.
[28] T. Sim, S. Baker, and M. Bsat, "The CMU pose, illumination, and expression (PIE) database," presented at the IEEE Int. Conf. Automatic Face and Gesture Recognition, Washington, D.C., Mar. 2002.
[29] R. Gross, I. Matthews, and S. Baker, "Appearance-based face recognition and light-fields," *IEEE Trans. Pattern Anal. Mach. Intell.*, vol. 26, no. 4, pp. 449–465, Apr. 2004.